Effects of Hydrogen and Chloride Ions on Automobile Interstitial-Free Steel Corrosion

L.Q. Guo, D. Liang,* Y. Bai,* X.L. Miao,** L.J. Qiao,‡,* and A.A. Volinsky****

ABSTRACT

Effects of hydrogen and chloride ions on the corrosion behavior of interstitial-free steel were investigated. The anodic polarization tests show that the corrosion and pitting potentials decrease with the rise of both the charging current density and the chloride ions concentration. For a given chloride ion concentration, the increase of the charging current density makes the pitting and the corrosion potentials drop sharply. Under a given hydrogen charging current density, the drops of the pitting and corrosion potentials have an approximately linear relationship with the increase of the chloride ions' concentration. It indicates that the hydrogen and chloride ions can affect the corrosion behavior. From the salt fog tests, the growth and development of the rust and pits on the hydrogen-charged specimen are faster than that of the uncharged one, displaying that hydrogen can decrease the corrosion resistance in the chloride ions' environment.

KEY WORDS: chloride ions, hydrogen-charged, interstitial-free steel, pitting, polarization, rust

INTRODUCTION

Interstitial-free (IF) steel has been widely used in the automotive industry because of its excellent characteristics of deep formability and fatigue resistance.[1-2] As the main material of the automobile's body, IF steel usually suffers from atmospheric corrosion attack, since it must work in corrosive atmospheres, such as acid rain and dust, especially with the presence of the chlorine ion in freezing salt or ocean aerosphere. The corrosion induced by the chloride ions may lead to serious damage in a short time. The high susceptibility to atmospheric corrosion limits the automobile steel applications. Although the corrosion behavior of automobile IF steel remains a concern, little research has been conducted, especially concerning the atmospheric corrosion behavior.[3] Therefore, there is a long way to a satisfactory explanation of the corrosion processes under different conditions, especially in the chlorine ion environment. Moreover, the generation and adsorption of hydrogen are unavoidable in many practical industrial processes, such as cathodic protection, and the permeated hydrogen into the metal can influence the corrosion behavior of materials. Hydrogen effects on the corrosion behavior have been investigated.[4-10] Experimental evidence indicated that hydrogen can increase the corrosion rates of austenite and ferrite steels[4,11-12] and decrease the pitting resistance of some metals.[8,13-14] There were also several interesting studies focused on the effects of pH and chlorine ion on the corrosion behavior of stainless steel.[15-16] To our knowledge, however, there are no systematic studies of the hydrogen and chloride ions effects on the corrosion behavior of automobile IF steel.

The goal of the present work was to study the effect of hydrogen on the corrosion behavior of automobile IF steel in boric acid (H_3BO_3) buffer solution with

Submitted for publication: September 4, 2013. Revised and accepted: April 27, 2014. Preprint available online: May 22, 2014, http://dx.doi.org/10.5006/1126.

‡ Corresponding author. E-mail address: lqiao@ustb.edu.cn.
* Corrosion and Protection Center, Key Laboratory for Environmental Fracture (MOE), University of Science and Technology Beijing, Beijing 100083, People's Republic of China.
** CNNC Nuclear Power Operations Management Co., Ltd. Haiyan, 314300, China.
*** Department of Mechanical Engineering, University of South Florida, Tampa, FL 33620.

ISSN 0010-9312 (print), 1938-159X (online)
14/0000165/$5.00+$0.50/0

TABLE 1
Chemical Composition of Interstitial-Free Steel (wt%)

Elements	C	Cr	Mn	Ni	Cu	N	Si	Al	P	Ti	S
Content	0.0014	0.015	0.42	0.014	0.016	0.0024	0.10	0.056	0.05	0.029	0.0066

different chloride ion concentrations. Electrochemical behavior of the IF steel was investigated by the potentiodynamic measurements, while optical microscopy was used to detect the surface morphology changes in the salt fog corrosion test to reveal the effects of hydrogen and chloride ions on the corrosion behavior.

EXPERIMENTAL PROCEDURES

Material and Sample Preparation

The experimental material was conventional IF steel, whose chemical composition is given in Table 1. The specimen was machined into square sheets with 20 by 20 by 1 mm dimensions. The surface of each specimen was wet ground with silicon carbide (SiC) paper up to 2000 grit, polished using diamond paste to 0.5 μm, and then ultrasonically cleaned in acetone (CH_3COCH_3) and ethanol (C_2H_5OH).

Hydrogen Charging

The hydrogen charging was conducted at room temperature in the 0.5 M sulfuric acid (H_2SO_4) aqueous solution for 3 h with an addition of 0.25 g/L arsenic trioxide (As_2O_3) as a hydrogen recombination poison to promote the absorption of hydrogen. During the hydrogen charging, specimens acted as the cathode, and the anode was a platinum mesh electrode with a size of 1 in by 1.5 in. The anode was parallel to the surface of the specimen to guarantee a uniform distribution of the charging current. To obtain samples with different hydrogen concentrations, the specimens were charged at different current densities (0.1, 1, and 10 mA/cm^2). After charging, the specimens were lightly polished using diamond paste and cleaned in acetone.

For the salt fog corrosion test, the specimens were charged in the 0.5 mol/L H_2SO_4 + 0.25 g/L As_2O_3 solution. The charging current density was 1 mA/cm^2 and the time of hydrogen charging was 30 min. After charging, specimens were ultrasonically cleaned in acetone and ethanol.

The hydrogen concentration in the specimen charged at different current densities (0.1, 1 and 10 mA/cm^2) was measured using a hydrogen analyzer by heating the charged and dried specimens to 600°C. Each hydrogen concentration was acquired experimentally at least five times.

Electrochemical Testing

A potentiostat were used to perform the electrochemical measurements. The specimen embedded in epoxy resin acts as a working electrode. To avoid crevice corrosion, the interface between the specimen and the resin were sealed by a special silica gel sealant. The exposed electrode surface area was 10 mm^2. All potentials were measured against a saturated calomel electrode (SCE), and the counter electrode was platinum foil. The electrochemical testing solution is a H_3BO_3 buffer solution, which consisted of 0.02 mol/L H_3BO_4, 0.005 mol/L $Na_2B_4O_7{\cdot}10H_2O$ solution, and NaCl with different concentrations (0, 5, 10, and 15 ppm). Prior to measurements, the working electrodes were immersed in the chloride-ion-free buffer solution for 30 min to make the corrosion potential of specimens stable. The polarization curves were recorded potentiodynamically at room temperature (25°C) under a scan rate of 20 mV/min from 70 mV (the corrosion potential) to the pitting potential.

Atmosphere Salt Corrosion Test

The atmosphere corrosion tests of the hydrogen-charged and the uncharged specimens were performed in a 5% NaCl salt fog chamber. After immersion in the salt fog chamber for 10, 30, or 40 min, the specimens were taken out and observed with an optical microscopy. The rust layers on the hydrogen-charged and the uncharged specimens were compared after the immersion test, which took place in the salt fog chamber for 24 h.

RESULTS

Effects of Hydrogen and Chloride Ions on Polarization Curves

Figure 1 shows typical polarization curves for the uncharged specimens and the specimens charged at 0.1, 1, and 10 mA/cm^2 in H_3BO_3 buffer solution with different NaCl concentrations. Despite the concentration of chloride ions, increasing the charging current density shifts the corrosion potential and the pitting potential to more negative values, i.e., weakening the corrosion resistance. Meanwhile, with increasing the hydrogen charging current density, the passive current density values elevate, meaning that the corrosion resistance of the passive film becomes worse. Figure 1 shows that the passive film breakdown occurs at a lower anodic potential in the hydrogen-charged specimen than that in the uncharged specimen. Moreover, with the increasing hydrogen charging current density, the pitting potential decreases and the anodic current density in the passive regions elevates, which is in an agreement with the

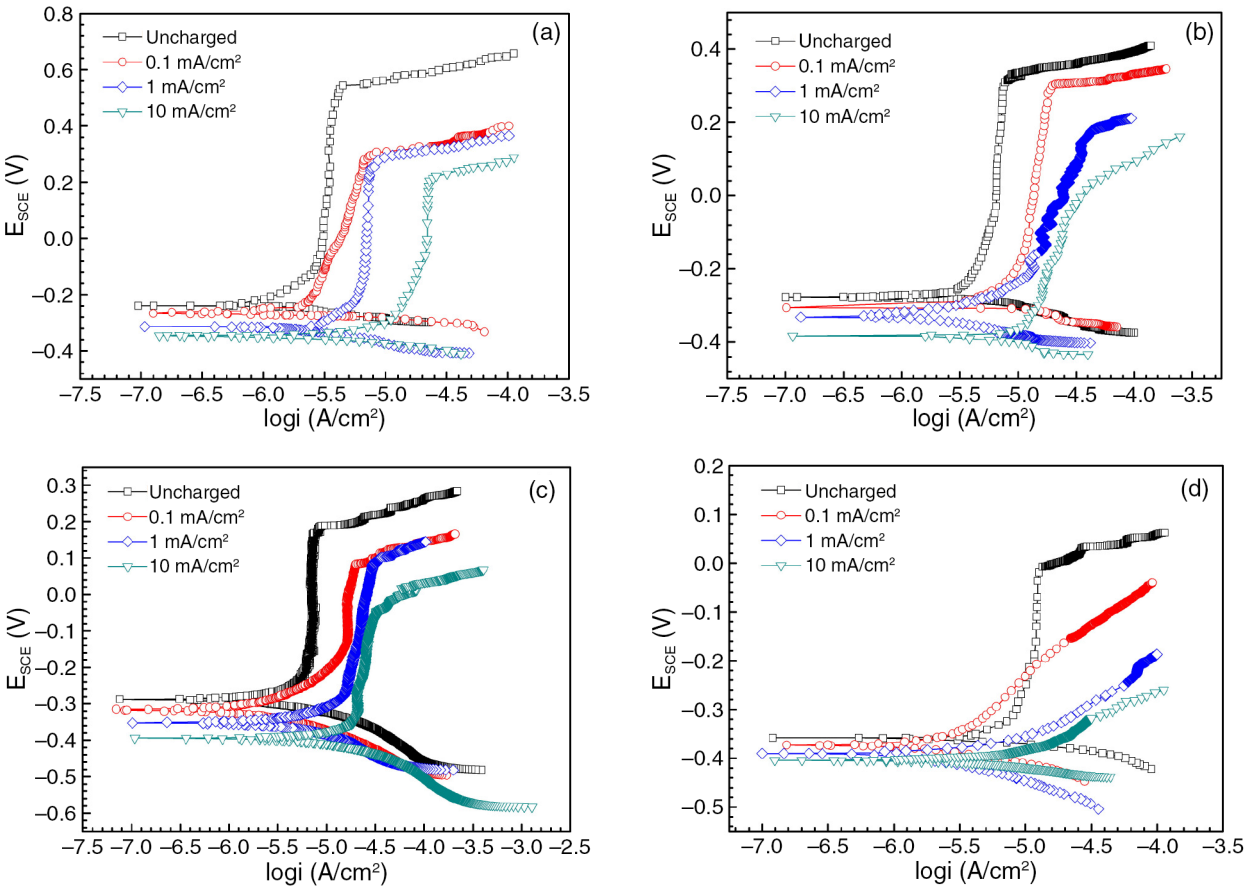

FIGURE 1. *Potentiodynamic polarization curves of uncharged and hydrogen-charged specimens at different charging densities in the boric acid buffer solution with different chloride ion concentrations: (a) 0 ppm, (b) 5 ppm, (c) 10 ppm, and (d) 15 ppm.*

TABLE 2
Hydrogen Concentration in Hydrogen-Charged Specimens at Different Charging Densities

	Hydrogen Concentration (ppm)	
Hydrogen Charging Density	**Hydrogen Concentration After Hydrogen Charging**	**Hydrogen Concentration Before Corrosion Testing**
0.1 mA/cm²	2.01±1.01	1.83±1.10
1 mA/cm²	7.81±3.5	6.84±2.77
10 mA/cm²	11.46±1.40	9.77±0.82

literature results.[9] It is also found that the corrosion potential and the pitting potential of the hydrogen-charged specimens become more negative with increasing chloride ion concentration, and this phenomenon is more pronounced in the solution with high NaCl concentration. The corrosion potential for the uncharged specimen varies from –239 mV (0 ppm chloride ion) to –357 mV (15 ppm chloride ion), while for the specimens charged with 10 mA/cm² changes from –345 mV (0 ppm chloride ion) to –404 mV (15 ppm chloride ion). The corrosion and pitting potentials in the solution with 15 ppm chloride ion decrease sharply. For the hydrogen-charged specimens, the only active process appears in the anodic polarization curves, while for the uncharged specimen, there is still a passivation process, as seen in Figure 1(d). Table 2 summarizes the hydrogen concentrations in hydrogen-charged specimens at different charging densities after hydrogen charging and immediately prior to corrosion testing. It can be seen that the hydrogen concentration increases with increasing hydrogen charging current density. These results indicate that either hydrogen or chloride ions affect the corrosion behavior of the IF steel, and both effects can lead to more severe corrosion.

Tables 3 and 4 summarize the corrosion and the pitting potentials of the specimens. Figures 2 and 3 show the relations between the concentration of chloride ions and the pitting potentials and the corrosion potentials, respectively. It can be seen clearly that the drops of the corrosion and pitting potentials have an approximately linear relationship with the chloride ions' concentration increase. In particular, with the increase of the concentration of chloride ions, the pitting potential decreases more sharply in the hydrogen-charged specimens than in the uncharged

TABLE 3

Corrosion Potential Values (E_{corr}/mV_{SCE}) of the Specimens Obtained from Potentiodynamic Polarization Curves in the Boric Acid Buffer Solution

Hydrogen Charging Density	NaCl Concentration			
	0	5 ppm	10 ppm	15 ppm
Without H	–239	–277	–287	–357
0.1 mA/cm^2	–267	–306	–341	–372
1 mA/cm^2	–314	–331	–352	–390
10 mA/cm^2	–345	–383	–394	–404

TABLE 4

Pitting Potential Values of Specimens Obtained from Potentiodynamic Polarization Curves in the Boric Acid Buffer Solution (E_{pit}/mV_{SCE})

Hydrogen Charging Density	NaCl Concentration			
	0	5 ppm	10 ppm	15 ppm
Without H	544	331	187	–7
0.1 mA/cm^2	363	280	114	—
1 mA/cm^2	248	182	79	—
10 mA/cm^2	204	84	16	—

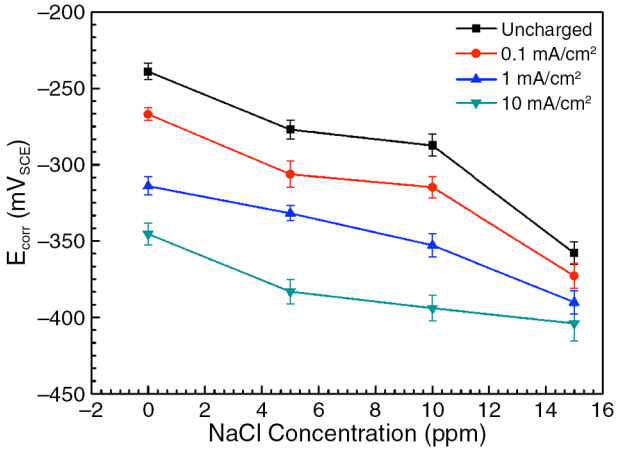

FIGURE 2. *Relationship between the concentration of chloride ions in boric acid buffer solution and corrosion potentials for the uncharged and hydrogen-charged specimens at different charging current densities.*

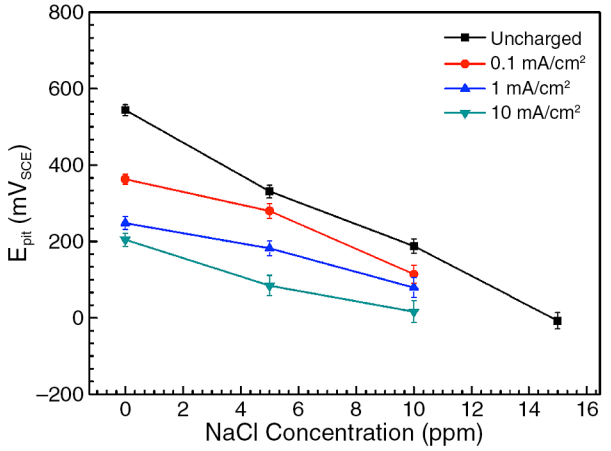

FIGURE 3. *Relationship between the concentration of chloride ions in boric acid buffer solution and pitting potentials for the uncharged and hydrogen-charged specimens at different charging current densities.*

one. The greater the hydrogen charging current density, the faster the pitting potentials drop. It should be stressed that higher concentrations of chloride ions and hydrogen imply lower corrosion and pitting potentials, i.e., a more difficult passivation process. In other words, the corrosion resistance of the IF steel obviously deteriorates with the increasing chloride ions' concentration or hydrogen concentration.

Effects of Hydrogen and Chloride Ions on Rust Corrosion

Figure 4 shows the morphology of the uncharged and hydrogen-charged specimens before (Figures 4[a] and [b]) and after immersion in a 5% NaCl salt fog chamber for different times (Figures 4[c] through [j]). After 10 min immersion in the NaCl salt fog, brown rust spots form on the surface of either the uncharged or the hydrogen-charged specimens; however, there are larger rust spots for the hydrogen-charged specimen, as seen in Figures 4(c) and (d). After additional immersion of 30 min, brown rust spots appear on the uncharged specimen (Figure 4[e]), while for the hydrogen-charged specimen, the brown rust flakes and silver corrosion products can be observed, which nearly cover the whole specimen surface (Figure 4[f]). As the immersion time increases past 40 min, the rust layer does not change on the uncharged specimen until 24 h (Figures 4[c], [e], [g], and [i]). However, for the hydrogen-charged specimen, after immersion for 40 min, the rust layer and the corrosion products spread almost all over the entire surface, and the massive brown rust layer grows, as seen in Figure 4(h). With the immersion time longer than 24 h, the surface of the hydrogen-charged specimen becomes completely covered with dark red rust (Figure 4[j]), while the surface of the uncharged specimen is cleaner than that of the hydrogen-charged specimen after 40 min immersion. To characterize the development of pits, the rust layers were removed and the cross-sectional images were observed. Figures 4(k) and (l) show the pit line depth profiles of Figures 4(i) and (j), revealing the pit depths on the hydrogen-charged and uncharged specimens. It is indicated that the pit depth on the hydrogen-charged specimen is larger than that of the uncharged one. These results show that the corrosion is faster in the hydrogen-charged specimen, which matches the polarization curve results in Figure 1, where hydrogen charging decreases the corrosion and pit potentials in the chloride ion environment.

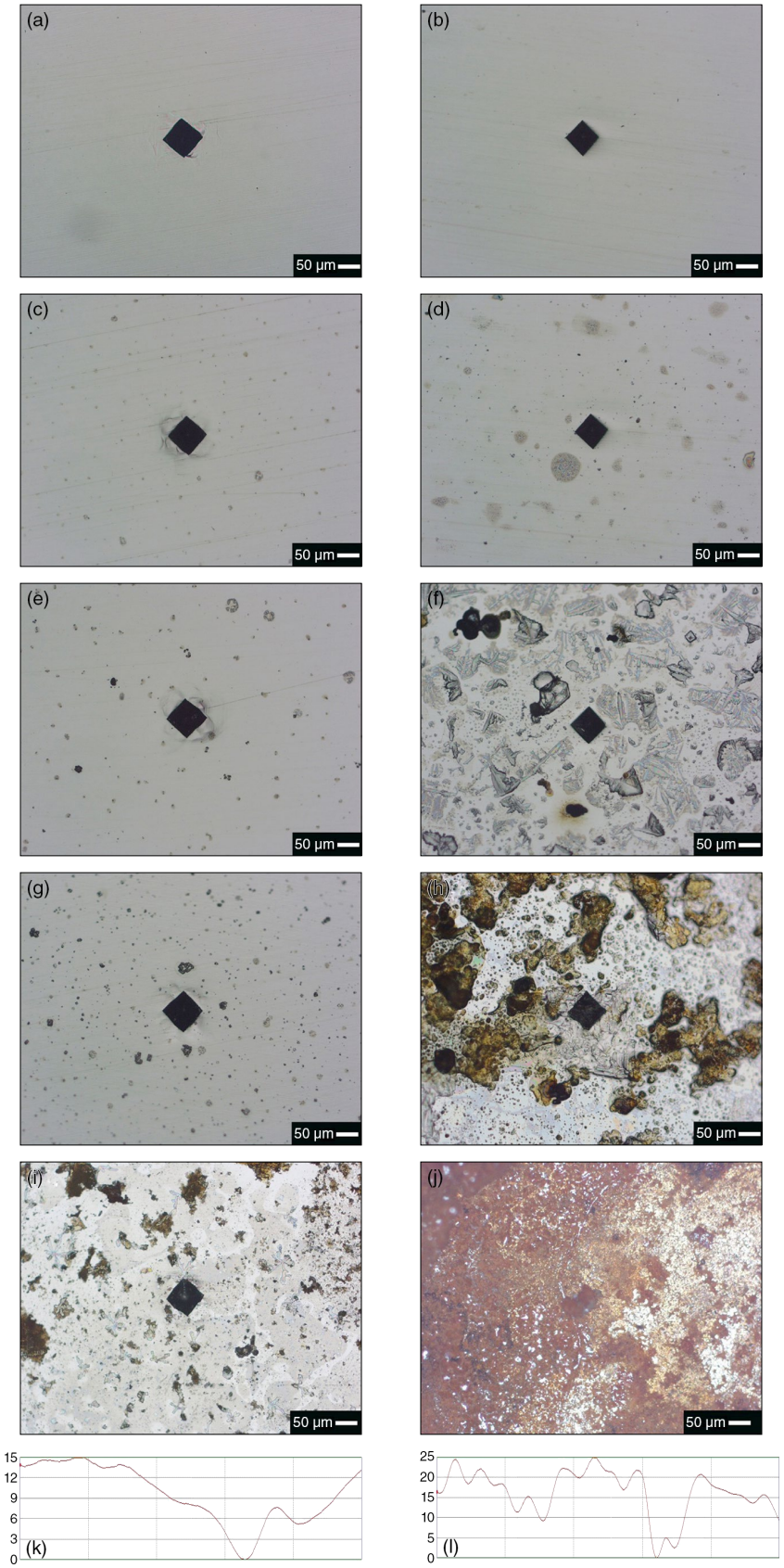

FIGURE 4. *Optical microphotographs of the IF steel specimens uncharged (left) and H-charged (right) (a, b) before and after immersion in a 5% NaCl salt fog chambers for (c, d) 10 min, (e, f) 30 min, (g, h) 40 min, and (i, j) 24 h, respectively. The (k) and (l) pit depth profile of the line shown in (i, j).*

DISCUSSION

The salt fog test shows that corrosion is faster in the hydrogen-charged specimen and becomes more severe with the immersion time, where hydrogen promotes the growth and development of the rust layer and pits in the chloride ion environment. This is consistent with the potentiodynamic polarization measurements, where the corrosion and pit potentials of the IF steel decrease with the concentration of hydrogen or chloride ions. It is reasonable to deduce that these results have been caused by the effect of hydrogen on the interface between the electrolyte and the electrode.[15] In a 5% NaCl salt fog chamber, a thin NaCl electrolyte film forms on the specimen surface, and local anode and cathode regions can form, causing corrosion. The dominating electrochemical reactions are iron dissolution (anodic reaction) and oxygen reduction (cathodic reaction):

$$Fe \rightarrow Fe^{2+} + 2e^{-} \quad (1)$$

$$O_2 + 2H_2O + 4e^{-} \rightarrow 4OH^{-} \quad (2)$$

The Fe^{2+} ions generated by the anodic reaction (Equation [1]) reacted with chloride ions that migrated to the anode to maintain charge neutrality, forming ferrous chloride ($FeCl_2$),[17-19] and reacted with OH^-, which was generated by the cathodic reaction (Equation [2]), forming ferrous hydroxide ($Fe[OH]_2$). Hydrogen, existing in the atomic form in metal, diffuses from the charged electrode during the anodic oxidation, and is oxidized to a proton.[20-22] Therefore, the chemical environment at the electrode and the electrolyte interface is changed after the electrode is pre-charged with hydrogen;[15] i.e., the oxidation of hydrogen in the IF steel decreases the pH at the interface. The lower the pH of the solution is, the more the electrode is attacked.[10,23] It was reported that the chloride ion can accelerate the pH drop at the local anode site in the atmospheric corrosion of steel.[24] The hydrogen protons can accumulate the chloride ions' adsorption at the local anode site in the chloride environment, which triggers the pH decrease at these anode sites;[24] therefore, the corrosion resistance reduces and more severe corrosion occurs in the hydrogen-charged specimen. On the other hand, hydrogen significantly increases the dissolution rate of Fe in stainless steel and their dissolution rates increase with increasing hydrogen charging current density,[4] leading to more corrosion attack. Therefore, the hydrogen and chloride ions can cause more severe corrosion behavior.

It is found that hydrogen and chloride ions can synergistically decrease the breakdown potential of the IF steel (Figures 1 through 3). Various models have been proposed to explain the pitting phenomena, such as the point defect model,[25] assuming that the chloride ion in solution would increase the cation vacancy/oxygen vacancy concentration in the passive film. Experimental evidence has revealed that the concentration of oxygen vacancies at the passive film surface is higher for the hydrogen-charged specimen.[10] Therefore, for the passive film on a hydrogen-charged specimen in a chloride-containing solution, the absorption of chloride ions into oxygen vacancies is accelerated, promoting the rate of cation vacancies; hence, the density of localized acceptor states is higher than that in the uncharged specimen.[10] As a result, the passive film is more easily broken in the hydrogen-charged specimen in a chloride-containing solution, and the pitting is formed more easily. This is confirmed in Figure 1; the breakdown potential of passive film is lower for the hydrogen-charged specimen. The critical concentration of chloride ion for the breakdown of a passive film decreases with the increasing hydrogen-charging current density, while the critical hydrogen-charging current density for the film breakdown decreases with chloride ion concentration (Figure 1). Moreover, as the chloride ion concentration increases to a critical value, there is no passivation processes in the polarization curves of the hydrogen-charged specimens, but there is still a passivation process for uncharged specimens (Figure 1[d]). It is mainly because the detachment of a passive film from the metal becomes easier for the hydrogen-charged specimens in chloride-containing solutions.[9,26-28]

Another reason for the effects of hydrogen and chloride ions on the pitting corrosion behavior may be that hydrogen charging changes the chemical compositions of the passive film.[10,14,29-31] Hydrogen in passive film exists in proton form, and the reaction of protons with O^{2-} increases the ratio of OH^-/O^{2-} in the passive films.[32-33] Moreover, chloride ions can easily displace OH^- ions in the passive film.[34] Therefore, with the increase of the concentration of hydrogen and chloride ions, the ratio of OH^-/O^{2-} in the passive film increases, which promotes the substitutions of OH^- ions by chloride ions and decreases the pitting resistance of the film.[35] It implies that the passive film containing hydrogen is degraded because of a higher concentration of defects, and is therefore more susceptible to corrosion attack. Experimental results indicated that there is a synergic effect between hydrogen and chloride ions.[36] The higher the concentration of hydrogen, the more susceptible the passive film is to attack by chloride ions.

CONCLUSIONS

❖ The hydrogen and chloride ions effects on the corrosion behavior of automobile IF steel was studied by potentiodynamic measurement and the salt fog test. The electrochemical measurement shows that the pitting potential and the corrosion potential decrease with the increases of the concentration of hydrogen

or chloride ions. Moreover, as the concentration of hydrogen or chloride ions increases to a critical value, the passivation processes of IF steel disappear in H_3BO_3 buffer solution. For a given chloride ion concentration, the increase of the charging current density makes the pitting potential and the corrosion potential drop sharply. Under a given hydrogen charging current density, the drops of the pitting potential and corrosion potential have an approximately linear relationship with the increase of the concentration of chloride ions. It indicates that hydrogen and chloride ions can affect the corrosion behavior of IF steel. From the salt fog test, the rust corrosion and pit corrosion are faster in the hydrogen-charged specimen, displaying that hydrogen promotes the growth and development of the rust layer and pits in the chloride ion environment.

ACKNOWLEDGMENTS

The authors acknowledge support from the National Natural Science Foundation of China under Grants nos. 51271026 and 51161160563.

REFERENCES

1. S.Q. Cao, J.X. Zhang, J.S. Wu, J.G. Chen, *Scr. Mater.* 52 (2005): p. 25-28.
2. I.G. Rodionova, E.T. Shapovalov, M.E. Kovalevskaya, *Metallurgist* 49 (2005): p. 314.
3. B. Hadzima, M. Janecek, Y. Estrin, H.S. Kim, *Mater. Sci. Eng., A* 462 (2007): p. 243-246.
4. L.J. Qiao, J.L. Luo, *Corrosion* 54 (1998): p. 281-288.
5. S. Pyun, C. Lim, R.A. Oriani, *Corros. Sci.* 33 (1992): p. 437-443.
6. H. Yashiro, B. Pound, N. Kumagai, K. Tanno, *Corros. Sci.* 40 (1998): p. 781-786.
7. M.Z. Yang, J.L. Luo, Q. Yang, L.J. Qiao, *J. Electrochem. Soc.* 146 (1999): p. 2107-745.
8. J.G. Yu, J.L. Luo, P.R. Norton, *Electrochim. Acta* 47 (2002): p. 1527-1534.
9. Q. Yang, J.L. Luo, *Electrochim. Acta* 45 (2000): p. 3927-3937.
10. Q. Yang, J.L. Luo, *J. Electrochem. Soc.* 148 (2001): p. B29-B39.
11. M. Hasegawa, M. Osawa, *Corrosion* 39 (1983): p. 115-120.
12. A.A. Seys, M.J. Brabers, A.A. Van Haute, *Corrosion* 30 (1974): p. 47-56.
13. Q. Yang, L.J. Qiao, S. Chiovelli, J.L. Luo, *Corrosion* 54 (1998): p. 628-634.
14. H. Yashiro, B. Pound, N. Kumagai, K. Tanno, *Corros. Sci.* 40 (1998): p. 781-786.
15. Y. Yuan, L. Li, C. Wang, Y.Y. Zhu, *Electrochem. Commun.* 12 (2010): p. 1804-1807.
16. H. Luo, C.F. Dong, X.G. Li, K. Xiao, *Electrochim. Acta* 64 (2012): p. 211-220.
17. V. Novokshchenov, *Corrosion* 50 (1994): p. 477-485.
18. M.A. Almomani, C.R. Aita, *J. Vac. Sci. Technol., A* 27 (2009): p. 449-454.
19. S.G. Li, L.H. Hihara, *J. Electrochem Soc.* 159, 4 (2012): p. C147-C154.
20. M. Hasegawa, M. Osawa, *Corrosion* 39 (1983): p. 115-120.
21. R. Ruetschi, R. Giovanoli, *J. Electrochem. Soc.* 145 (2001): p. 2663-2670.
22. P. Ruetschi, R. Giovanoli, *J. Electrochem. Soc.* 135 (1988): p. 2661-2667.
23. M. Li, L.Q. Guo, L.J. Qiao, Y. Bai, *Corros. Sci.* 60 (2012): p. 76-81.
24. T. Kamimura, K. Kashima, K. Sugae, H. Miyuki, T. Kudo, *Corros. Sci.* 62 (2012): p. 34-41.
25. D.D. Macdonald, *J. Electrochem. Soc.* 139 (1992): p. 3434-3439.
26. J.G. Yu, J.L. Luo, P.R. Norton, *Langmuir* 18 (2002): p. 6637-6645.
27. Y.M. Zeng, J.L. Luo, P.R. Norton, *Electrochim. Acta* 49 (2004): p. 703-714.
28. H.P. Kim, R.H. Song, S.I. Pyun, *Corros. Sci.* 23 (1998): p. 254-259.
29. J.G. Yu, C.S. Zhang, J.L. Luo, P.R. Norton, *J. Electrochem. Soc.* 150 (2003): p. B68-B75.
30. J.G. Yu, C.S. Zhang, J.L. Luo, P.R. Norton, *J. Electrochem. Soc.* 150 (2003): p. B405-B411.
31. Y.M. Zeng, J.L. Luo, P.R. Norton, *Thin Solid Films* 460 (2004): p. 116-124.
32. P. Ruetschi, R. Giovanoli, *J. Electrochem. Soc.* 135 (1988): p. 2663-2670.
33. M.E. Armacanqui, R.A. Oriani, *Corrosion* 44 (1988): p. 698-705.
34. P. Marcus, J.M. Herbelin, *Corros. Sci.* 34 (1993): p. 1123-1128.
35. R.H. Song, S.U. Pyun, R.A. Oriani, *J. Electrochem. Soc.* 137 (1990): p. 1703-1710.
36. S. Pyun, C. Lim, R.A. Oriani, *Corros. Sci.* 33 (1992): p. 437-440.